

Multiple conduction paths in boron δ -doped diamond structures

Niall Tumlity,¹ Joseph Welch,¹ Haitao Ye,¹ Richard S. Balmer,² Christopher Wort,^{2,3} Richard Lang,³ and Richard B. Jackman^{1,a)}

¹Department of Electronic Engineering and London Centre for Nanotechnology, University College London, 17-19 Gordon Street, London WC1H 0AH, United Kingdom

²Element Six Ltd., Kings Ride Park, Ascot, Berkshire SL5 8BP, United Kingdom

³Diamond Microwave Devices (DMD) Ltd., Kings Ride Park, Ascot, Berkshire SL5 8BP, United Kingdom

(Received 11 November 2008; accepted 7 January 2009; published online 4 February 2009)

Impedance spectroscopy has been used to investigate conductivity within boron-doped diamond in an intrinsic/delta-doped/intrinsic (i - δ - i) multilayer structure. For a 5 nm thick delta layer, three conduction pathways are observed, which can be assigned to transport within the delta layer and to two differing conduction paths in the i -layers adjoining the delta layer. For transport in the i -layers, thermal trapping/detrapping processes can be observed, and only at the highest temperature investigated (673 K) can transport due to a single conduction process be seen. Impedance spectroscopy is an ideal nondestructive tool for investigating the electrical characteristics of complex diamond structures. © 2009 American Institute of Physics. [DOI: 10.1063/1.3075860]

Diamond is considered to be an ideal material for the fabrication of high performance electronic devices if problems associated with poor material quality and doping can be overcome.¹ Recent single crystal diamond layers grown by plasma-enhanced chemical vapor deposition (CVD) have been shown to display carrier mobility values that surpass those of the very best natural diamond stones.² Doping remains a more significant problem; boron forms a p -type acceptor with an activation energy (E_a) of 0.37 eV, meaning that few holes are present at room temperature.³ Borst and Weiss⁴ showed that when $[B] > 10^{18} \text{ cm}^{-3}$, this energy sharply declines, as a boron impurity band emerges, with concentrations greater than 10^{19} cm^{-3} , leading to semimetallic characteristics. While this removes the problem associated with the E_a of the acceptors, the conduction mechanism has now become “hopping” with the associated extremely low values of carrier mobility. A solution may be the use of δ -doping, where a highly boron-doped layer with nanometer dimensions is sandwiched between undoped materials. The heavily doped δ -region will provide carriers with little thermal activation, while the carriers will emerge from this layer and be transported through the (higher mobility) intrinsic layers each side. A number of reports of the growth of such structures and their use for the formation of field-effect transistors (FETs) have been made and this work has been reviewed.^{5,6} The ideal δ -layer thickness would be 1–2 nm.⁷ Given the nature of the CVD process used this is technologically challenging. Aleksov *et al.*⁷ reported a thickness of 6 nm, although recently the same group achieved 1.1 nm,⁸ corresponding to around three atom layers of doped diamond.

It is essential to be able to determine the electronic characteristics of the δ -layer and the surrounding intrinsic material if effective FETs are to be designed. Hall effect measurements can provide carrier concentrations and mobility values, but understanding the contribution of each region to the numbers determined this way is difficult. Aleksov *et al.*⁷ reported a method whereby repeated etching-measurement

cycles were used to study the an i - δ - i structure, revealing an activation energy of 30 meV within the δ and 1.5 eV outside. However, this approach is time-consuming, limited in depth resolution by the etching process, and destructive of the layers. In this letter we report on the use of impedance spectroscopy (IS) for determining conduction paths within complex diamond i - δ - i structures and their characteristics.

Microwave plasma-enhanced CVD was used to produce both intrinsic and boron-doped layers on type Ib high pressure high temperature single crystal substrates using growth conditions for high quality materials similar to those described previously.² Following the growth of a 100 nm thick i -layer on the substrate, a δ -layer was grown with a full width at half maximum thickness of 5 nm as judged by secondary ion mass spectroscopy (SIMS). Onto the δ -layer was grown an intrinsic capping layer of 20 nm thickness. SIMS analysis showed $[B]$ in the δ -layer to be $\sim 5 \times 10^{20} \text{ atoms cm}^{-3}$. All samples were subjected to treatments that are known to leave the surface in a strongly oxidized state,⁹ avoiding so-called “surface conductivity.”¹⁰ Au contacts were evaporated onto the surface of the samples, which were then placed inside a vacuum chamber providing atmospheric control and electrical shielding during analysis. Measurements were made within the temperature range 300–900 K. IS was performed with a Solartron SI1260 with a high impedance input module 1296. The real and imaginary parts of the impedance were measured as a function of frequency (0.1 Hz–10 MHz) to produce “Cole–Cole” plots. Each contribution to the overall impedance of the sample can be characterized by an individual RC component and hence differing semicircular responses in the Cole–Cole plots. In practice these responses often overlay each other, meaning that careful fitting of the data to ideal semicircles is required.¹¹ The measurements are repeated as a function of temperature such that the activation energy for each conduction path can be determined.

Cole–Cole plots for a typical sample are shown in Figs. 1(a)–1(c) for increasing sample temperature (not all temperatures are included for brevity). In Fig. 1(a) the imaginary component of the impedance is plotted against the real component as a function of frequency at 300 K. Initial inspection

^{a)}Author to whom correspondence should be addressed. Electronic mail: r.jackman@ucl.ac.uk.

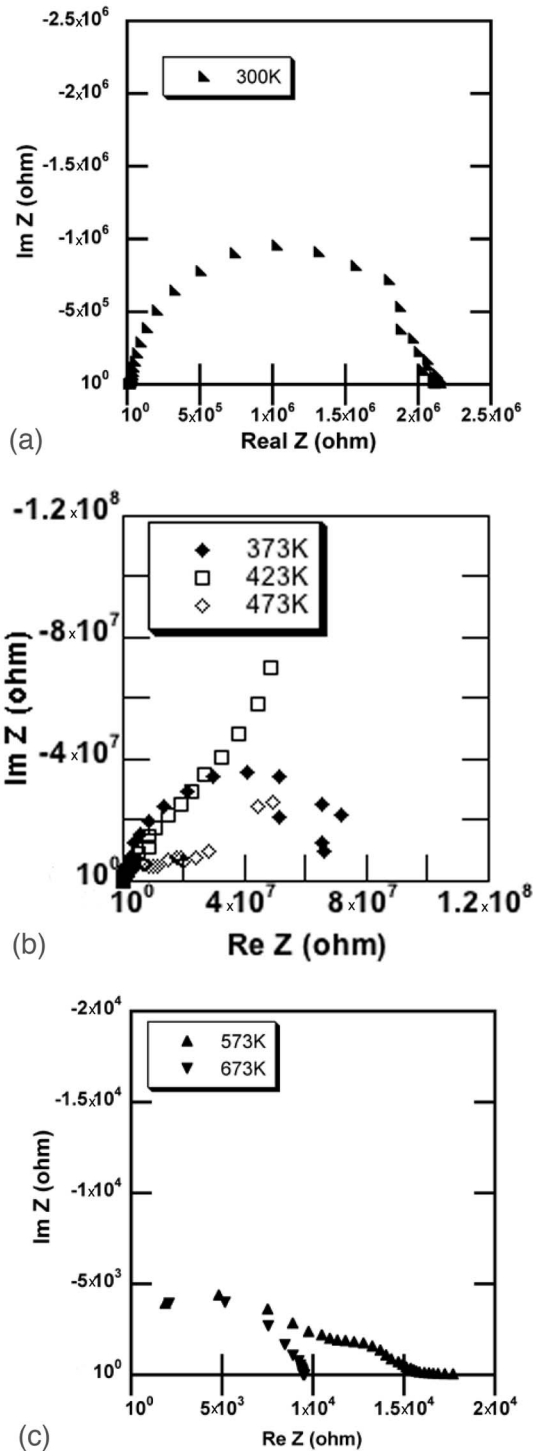


FIG. 1. Cole-Cole plots of real vs imaginary component of the impedance values determined as a function of frequency for measurements carried out at (a) 300 K, (b) 373–473 K, and (c) 573–673 K.

of the graph suggests the presence of a single semicircular response, while in Fig. 1(b) the situation is clearly somewhat more complicated once the temperature has increased. First, the inspection of the values on the axes shows that the film has become *more resistive* as the temperature increases from 300 to 373 K. Further, the shape of the response has altered. Moreover, impedance measurements for a temperature of 423 K show a further increase in resistance values and a rather dramatic change in the shape of the graph [Fig. 1(b)]. Also shown in Fig. 1(b) are the measurements obtained for a

TABLE I. Resistance and capacitance values determined for the three semicircular responses within the Cole-Cole plots measured at 373 K using curve fitting.

T (K)	Impedance	Semicircle 1	Semicircle 2	Semicircle 3
373	R (Ω)	13 223	9.7×10^6	8.6×10^7
373	C (F)	2×10^{-12}	3×10^{-11}	3×10^{-10}

temperature of 473 K. Intriguingly, the impedance values are now *lower* than those for 373 and 423 K, so the sample now becomes *less resistive* as the temperature further increases. This trend continues as the temperature is raised to 573 K [Fig. 1(c)] with little apparent change at 673 K. To confirm that these observations did not relate to the type Ib substrate underlying the i - δ - i structure, impedance measurements were obtained for a Ib crystal alone; the resistance remained considerably greater than that recorded here (at greater than $10^9 \Omega$) over this temperature range.

To model the RC components of each conduction path leading to the data shown in Fig. 1, it is necessary to fit semicircular responses to the data. A semicircular response can be fitted to the data before the curve rises steeply in value as the frequency decreases. A second semicircular response can then be fitted, followed by a third as the frequency is decreased further. Table I shows the R and C values that can be determined from these fits. In fact, while the magnitude and relative contributions vary with temperature, a similar analysis of all temperatures (including 300 K) up to 523 K showed the clear presence of three semicircular responses in all of the impedance measurements. However, the data presented in Fig. 1(c) for analysis at 673 K revealed only one semicircular response.

It is interesting to consider the way the resistance determined for each of these RC contributions changes with temperature such that an activation energy for each process can be determined. Figure 2 shows this data with the resistance of each plotted against $1/T$. It is immediately apparent that semicircle 1 has the lowest resistance and displays little variation in R with T ; an E_a of less than 20 meV can be proposed. In stark contrast the data points for both semicircular responses 2 and 3 show an increase in resistance with increasing temperature until peaking around 423 K, after which the resistance is seen to *decline* with increasing temperature. In the case of semicircular response 2, sufficient

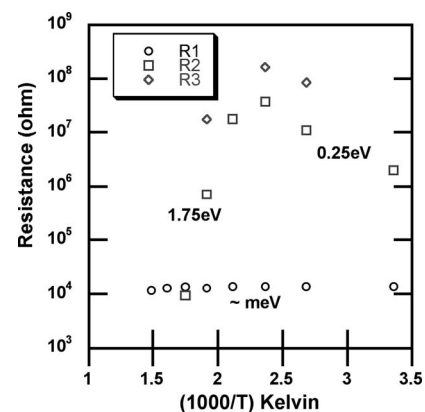


FIG. 2. Plot of resistance vs $1000/T$ to reveal the activation energy for the three conduction processes derived from temperature dependent Cole-Cole plots.

data points exist to determine that the activation energy for the initial increase in resistance with temperature is 0.25 eV, while the activation energy for the decreasing resistance as the temperature increases further is 1.75 eV.

IS has been previously used to characterize polycrystalline diamond films,^{12,13} where the contributions from the grains and grain boundaries were observed. The strength of the impedance technique lies in its ability to identify the individual components that contribute to the overall conductivity; we have previously shown that this can include different contributions to conduction within doped single crystal diamond,^{14,15} but the complexity of the current samples is unprecedented. The observation of three semicircular responses up to 523 K is interesting and suggests that three distinct conduction paths exist within this structure. It has been widely established that capacitance values in the picofarad range arise from ordered material, while contributions from disordered material are most normally observed to lie in the nanofarad region.¹¹ In the present case capacitance values for the highest frequency component are observed in the picofarad range, while the second and third semicircular components appear at higher capacitance values, 10 and 100 picofarad, respectively (Table I). This might suggest an increase in crystal disorder for these conduction paths. The contribution to the overall conduction that shows an activation energy of less than 20 meV is most likely to arise from the heavily boron-doped δ -layer, as this value is typical for doping levels in the region of 10^{20} cm⁻³ as we have here.⁴ That the resistance of this region is so low also agrees with this assignment. The other conduction paths that can be observed are considerably more resistive, implying that the carrier densities responsible are comparably low. That both of the other conduction paths display two activation energies with opposite signs is intriguing. To increase the resistance of the conduction path with increasing temperature implies that the carriers responsible are acquiring sufficient energy to become trapped at sites with an energy of some 0.25 eV from the valance band edge, assuming the process to be one of hole transport. At temperatures greater than 423 K, this trap state is emptied and the resistance begins to rapidly fall with increasing temperature. The thermal activation energy for the decrease is 1.75 eV. It is beyond the remit of this short letter to begin to assign the states that may give rise to these energies, but a logical proposal based upon the *i*- δ -*i* structure being investigated would be to propose that they arise from carrier transport within the (defective) interfacial regions between the intrinsic material and the heavily doped diamond layer. That two distinct conduction pathways can be determined would be most easily explained if transport in the interface between the *i*-layer under the heavily doped diamond differed from that in the capping *i*-layer above it. This might be anticipated as epitaxial growth of *i*-diamond onto such a heavily doped layer could easily lead to an interface that differs from that achieved when a heavily doped boron

layer is grown on an already present high quality diamond region. This could also explain the fact that these two conduction paths differ in capacitance value by an order of magnitude (Table I), which may arise if one has a higher level of crystal disorder than the other. In the current case, at 673 K only one semicircular response can be seen [Fig. 1(c)]. The capacitance value for this single semicircle is in the picofarad range, and the resistance is very low. These facts suggest that at this temperature only a single conduction path is active. This may be because all interfacial traps are emptied at this high temperature and carriers are free to move within a single channel. It is not possible from this data alone to suggest whether carrier transport at this point is solely within the delta-layer or the adjoining (now uncharged) *i*-layers.

In summary, we have demonstrated that IS is a powerful tool for investigating conduction paths within complex multilayer structures fabricated from diamond, such as the *i*- δ -*i* structure studied here. It has been shown that the technique is sensitive to differences in the transport characteristics displayed by the two different interfacial regions, in addition to conduction within the δ -layer itself. It is clear that the use of IS, when allied to other characterization tools, can provide an excellent, nondestructive method for optimizing these types of complex diamond structures.

This work was carried out as part of a contract to UCL from Diamond Microwave Devices Limited (DMD), for which DMD had received funding from MBDA UK Ltd., and the UK MoD (DTIC), which also funded the provision of *i*- δ -*i* material from Element Six Ltd.

¹Diamond: *Electronic Properties and Applications*, edited by L. Pan and D. Kania (Kluwer, Boston, 1995).

²J. Isberg, J. Hammersberg, E. Johansson, T. Wikstro, D. J. Twitchen, A. J. Whitehead, S. E. Coe, and G. A. Scarsbrook, *Science* **297**, 1670 (2002).

³N. Fujimori, H. Nakahata, and T. Imai, *Jpn. J. Appl. Phys., Part 1* **29**, 824 (1990).

⁴T. H. Borst and O. Weiss, *Phys. Status Solidi A* **154**, 423 (1996).

⁵A. Aleksov, A. Denisenko, M. Kunze, A. Vescan, A. Bergmaier, G. Dollinger, W. Ebert, and E. Kohn, *Semicond. Sci. Technol.* **18**, S59 (2003).

⁶A. Aleksov, M. Kubovic, N. Kaeb, U. Spitzberg, A. Bergmaier, G. Dollinger, Th. Bauer, M. Schreck, B. Stritzker, and E. Kohn, *Diamond Relat. Mater.* **12**, 391 (2003).

⁷A. Aleksov, A. Vescan, M. Kunze, P. Gluche, W. Ebert, E. Kohn, A. Bergmaier, and G. Dollinger, *Diamond Relat. Mater.* **8**, 941 (1999).

⁸H. El-Hajj, A. Denisenko, A. Bergmaier, G. Dollinger, M. Kubovic, and E. Kohn, *Diamond Relat. Mater.* **17**, 1259 (2008).

⁹B. Baral, S. S. M. Chan, and R. B. Jackman, *J. Vac. Sci. Technol. A* **14**, 2303 (1996).

¹⁰O. A. Williams and R. B. Jackman, *J. Appl. Phys.* **96**, 3742 (2004).

¹¹A. Huanosta and A. R. West, *J. Appl. Phys.* **61**, 5386 (1987).

¹²H. Ye, O. A. Williams, R. B. Jackman, R. Rudkin, and A. Atkinson, *Phys. Status Solidi A* **193**, 462 (2002).

¹³H. T. Ye, R. B. Jackman, and P. Hing, *J. Appl. Phys.* **94**, 7878 (2003).

¹⁴H. T. Ye, O. Gaudin, R. B. Jackman, P. Muret, and E. Gheeraert, *Phys. Status Solidi A* **199**, 92 (2003).

¹⁵S. Curat, H. Ye, O. Gaudin, R. B. Jackman, and S. Koizumi, *J. Appl. Phys.* **98**, 073701 (2005).